

# Mushroom-like eddy dipoles in the Brazil Current: genesis and dynamics diagnostics using a regional ocean model

L. Calado <sup>a,\*</sup>, R. Domingues <sup>b,c</sup> A. Gangopadhyay <sup>d</sup>  
W. Watanabe <sup>e,a</sup>

<sup>a</sup>*Instituto de Estudos do Mar Almirante Paulo Moreira - IEAPM Marinha do Brasil, Rua Kioto 253, Praia dos Anjos, Arraial do Cabo - RJ,28930-000, Brazil.*

<sup>b</sup>*Cooperative Institute for Marine and Atmospheric Studies, University of Miami, 4600 Rickenbacker Causeway, Miami, FL 33149, USA*

<sup>c</sup>*Atlantic Oceanographic and Meteorological Laboratory, National Oceanic and Atmospheric Administration (NOAA), 4301 Rickenbacker Causeway, Miami, FL 33149, USA.*

<sup>d</sup>*School for Marine Science and Technology (SMAST) - University of Massachusetts Dartmouth, 285 Old Westport Road N. Dartmouth MA 02747.*

<sup>e</sup>*Instituto Oceanográfico da Universidade de So Paulo (IO-USP).*

---

## Abstract

The mesoscale dynamics of in the southeastern region of Brazil is dominated by Brazil Current (BC), which is permeated by features such as meanders and eddies. Some of these mesoscale features are recurring in time, and are often observed in pairs in the form of eddy dipoles that are sometimes referred as *Mushroom like eddies*. In this study we report the frequency at which these events occur, and investigate the main dynamic mechanisms driving the formation and evolution of these mesoscale features in the BC. To accomplish this, we combine the analysis of satellite data with numerical simulations targeting one event with average characteristics. The main finding from this study is that ... This is important because ...

*Key words:* Brazil Current, Mesoscale Features, Eddy Dipoles, Mushrooms-like Eddy Dipoles, Feature Models

---

\* Corresponding author.

*Email address:* leandro\_calado@hotmail.com (L. Calado).

# 1 Introduction

2 The circulation around the Brazilian coast can be considered complex and  
3 highly variable, because water moves in distinct directions in different verti-  
4 cal layers and because it's mesoscale activity. Figure 1 shows state-of-the-art  
5 knowledge of the main oceanographic features in this domain, from which the  
6 Brazil Current (BC) can be considered one of the most important. This cur-  
7 rent, along with the North Brazil Current (NBC) originates from the Southern  
8 Equatorial Current (SEC) bifurcation around 15°S [da Silveira et al., 2008;  
9 Soutelino et al., 2011].

10 The BC mesoscale activity is evident as a strong meandering south of the  
11 Vitoria Trindade Ridge (VTR) associated with described recurrent eddies,  
12 such as the Vitoria Eddy [Schmid et al., 1995], the Cabo de São Tomé Eddy  
13 (CSTE) and the Cabo Frio Eddy (CFE) [Calado et al., 2006] (Fig. 1). In the  
14 latter, the occurrence CFE is primarily linked with the abrupt change in the  
15 coastline orientation combined with the steepness bottom topography; south  
16 of Cabo Frio (CF) the BC detach the shelf break and flows inertially to deeper  
17 waters, developing potential vorticity and, thus, a cyclonic meander. The same  
18 dynamic reasoning also explains the meandering north of the Cabo de São  
19 Tomé (CST) [Silveira et al., 2000]. There, cyclonic and anticyclonic meanders  
20 alternate towards the Santos Basin, as a Rossby wave. As a consequence, the  
21 BC path shows strong variations in time [Garfield, 1990; Lorenzetti et al.,  
22 2009; da Silveira et al., 2008].

23 The mesoscale variability of the BC can often develop as the recurring cou-  
24 pling cyclonic and anticyclonic eddies. These features, Eddy dipoles, are often  
25 observed to develop at the BC region approximately at 23N, where a cyclonic  
26 meander of the BC usually develops due to a sharp change in the topographic  
27 slope orientation. Sometimes, these eddy dipoles can evolve as a mushroom-  
28 like eddy when the BC separates from the coast [Miranda 2013] (REFEREN-  
29 CIA??). These features are particularly of interest because they can steer the  
30 flow of the BC, which may have important consequences for offshore activi-  
31 ties and various bio-physical processes, since western boundary currents and  
32 eddies can be key components in the dispersal of larvae from commercially  
33 important fish species [e.g Domingues et al., 2016].

34 Mushrooms like currents or eddies, are possibly one of the most common  
35 mesoscale features in the oceans [Fedorov and Ginsburg [1986] In fact, la-  
36 grangian analysis of altimeter data using the Lyapunov exponent technique  
37 revealed that, indeed, eddy dipole signals are indeed commonly observed in  
38 the global oceans [Beron-Vera et al. 2008]. Eddy dipoles may form on regions  
39 dominated by intense currents, such as within the Gulf Stream, and also under  
40 weaker regimes, suggesting that the formation of these features does not de-

41 pend on the strength of the background flow [Hookers and Brown 1996]. In the  
42 BC region, idealized studies [Miranda, 2013] showed that that the formation  
43 of eddy dipoles along the BC seems to be linked with unstable wave trains  
44 that start when the BC detaches from the coast, suggesting the importance  
45 of barotropic instability mechanisms for the formation of the dipolar feature.  
46 Yet, a deeper understanding on the occurrence of eddy-dipoles in the BC, and  
47 on the processes driving their formation and evolution is still needed. This  
48 study aims to fulfill this gap.

49 In this study, we assess the occurrence of eddy dipoles events in the BC during  
50 1993-2014, focusing on underlying dynamics of one event with mean character-  
51 istics. It is hoped that our results and analysis will provide additional insight  
52 into the understanding of mechanisms driving the mesoscale variability of the  
53 BC, and into the overall understanding of the interaction of western bound-  
54 ary currents with mesoscale eddies. This manuscript is organized as follows:  
55 in section 2, we estimate the occurrence and overall characteristics of eddy  
56 dipoles in the BC; in section 3, we describe the data and numerical approach  
57 employed to investigate the dynamics of one specific eddy dipole event that  
58 had average characteristics; in section 4 modeling results are verified against  
59 available satellite data; section 5 focus on assessing the dynamical mechanisms  
60 driving the formation and evolution of a eddy dipole event based on model  
61 simulations; and section 6 describes the main conclusions and final remarks  
62 from this study.

## 63 **2 Eddy Dipoles in the BC during 1993-2014**

64 Eddy dipoles correspond to recurring mesoscale features at the Brazil Current  
65 region, and may play an important role on the total variability of this western  
66 boundary current. Using AVISO’s satellite altimetry record, dipole features  
67 may be identified as side-by-side eddy-like signals with positive and negative  
68 sea height anomaly values (SHA), which correspond to adjacent cyclonic and  
69 anticyclonic eddies, respectively. During 1993-2014, at least 62 events (Fig.  
70 3) were identified using the search criteria described above. These events ex-  
71 hibited no evident seasonally and persisted for 42–28 days, with the shortest  
72 event lasting 21 days, and the longest lasting 140 days, over 4 months. The  
73 eddy-like features associated with these events had average diameters of 150  
74 40 km, with values ranging between 90 km and 330 km.

75 This cyclonic meander eventually grows due to baroclinic instability mecha-  
76 nisms, originating the Cabo Frio Eddy (CFE) [Calado et al., 2006]. When the  
77 CFE, which integrates part of the coastal flank of the BC, encounters an an-  
78 ticyclonic feature originated in the ocean interior, an eddy dipole can form. A  
79 typical case developed in July 2006 (Fig. 3 a,b,c), when the CFE eddy encoun-

80 tered an anticyclonic feature of similar size on the offshore flank of the BC,  
81 forming a mushroom-like-eddy dipole. This type of eddy dipole constrains the  
82 flow of the BC between these two features, which then become symmetrically  
83 elongated as they are advected by the current to the south (Fig. 3 b,c). Figure  
84 3 shows other examples of dipole features that are also observed at the BC  
85 region, such as dipoles with inversed polarity (Fig. 3 d,e,f) and dipoles with  
86 asymmetric eddies. In the latter, the BC and the unbalanced vorticity between  
87 the two eddies causes a translation-type movement of the smaller eddy around  
88 the bigger eddy (Fig. 3 e,f).

89 In this study, focus is given to the event from July 2006, which corresponded  
90 to an average typical case of mushroom-like eddy dipoles in the BC, with  
91 the dipole being formed by eddies with diameters of 140 km, and the event  
92 itself lasting 45 days. In addition, available meteorological conditions at that  
93 time permitted satellites to capture enhanced quality high resolution satellite  
94 sea surface temperature (SST) imagery (Fig. 5). SST fields show how the  
95 interaction of the cyclonic feature with the anticyclonic causes the advection of  
96 warm waters from the BC, forming a mushroom-like eddy pattern. On the next  
97 few sections, our analysis focuses on assessing the existing ocean conditions  
98 during a period of one week, starting with the formation of the dipole from  
99 July 2006. To accomplish this, we employ a high resolution regional ocean  
100 model for the BC region. It is hoped that this analysis will provide additional  
101 knowledge about the formation and initial evolution of mushroom-like-eddy  
102 dipoles, and also about how these processes may affect the variability of the  
103 BC.

### 104 **3 The July 2006 event: data & numerical simulations**

#### 105 *3.1 Satellite SST data*

106 In order to assess the synoptic scenario in the BC during the July 2006 event,  
107 SST data were derived from the GOES 10-12 satellite, calibrated at the in-  
108 frared thermal band, for the period between July 23 and 28, 2006, which al-  
109 lowed a clear identification of the eddy dipole that developed into a mushroom-  
110 like eddy structure. The SST field from July 23 2006 was used to build the  
111 nowcast structure of the BC, while subsequent SST fields from July 24 to 28  
112 were used to verify numerical simulations used to investigate the underlying  
113 dynamics driving this feature.

114 The SST field from July 23 2006 (Fig. 5) show the thermal signature of a  
115 meandering BC, and of prominent eddy dipole near Cabo Frio. A dipole  
116 formation is evident, where the CFE is the cyclonic gire on the coastal side

117 of the current, along with an anticyclonic gire on the oceanic side. This SST  
118 field shows how warm surface waters carried by the BC are entrained into  
119 both cyclonic and anticyclonic eddies that form the dipole. This mushroom-  
120 like feature also forms an SST front centered at approximately 25.5°S that  
121 can be used to trace the evolution of this feature. The configuration of this  
122 mushroom-like-eddy structure were our target features for the development  
123 of numerical simulations, which intend to represent: (i) the BC, with well  
124 developed CF meander (eddy) and (ii) the anticyclonic eddy on the offshore  
125 edge of the BC.

### 126 3.2 *The Feature Model technique*

127 In order to simulate the dynamics of the mushroom-like eddy dipole observed  
128 on July 2006, we develop numerical simulations based on a Feature Model  
129 technique. The Feature Model technique was first described by Robinson et al.  
130 [1988] and can be considered a realistic way to simulate the oceanic thermo-  
131 haline structure in the lack of real oceanic data. Several studies employed this  
132 methodology in nowcasting, forecasting and data assimilation in the western  
133 North Atlantic [Fox et al., 1992; Gangopadhyay et al., 1997; Robinson and  
134 Glenn, 1999; Calado et al., 2008; Gangopadhyay et al., 2011]. It's philosophy  
135 is to build the three-dimensional structure of known oceanic features based on  
136 a parametric approach [Calado et al., 2008].

137 This study will follow the achievements of the methodology reported in Calado  
138 et al. [2008]. Below, we describe the steps of the Feature-oriented regional  
139 model system (FORMS) implementation, following the formulation presented  
140 on Gangopadhyay and Robinson [2002]. First, the in situ dataset used to  
141 develop the FORMS is presented, second the Feature Model conception is  
142 described, and third the description of modeling approach is presented to  
143 achieve the nowcast/forecast fields. Fig. 4 shows the steps within the FORMS  
144 methodology.

145 In order to prescribe the mesoscale features of interest, in this study it is  
146 employed data collected during several cruises from DEPROAS's ("Dinâmica  
147 do Ecossistema de Plataforma da Região Oeste do Atlntico Sul" - Ecosystem  
148 Dynamics of the Continental Shelf Region of the western South Atlantic) (for  
149 more information please refer to Silveira et al. [2004]; Calado et al. [2006,  
150 2008]). It includes data from the winter 2001 campaign, the summer 2002  
151 and winter and spring campaigns of 2003 . The main oceanographic features  
152 that are often observed in the southeastern Brazil coast were sampled during  
153 these cruises, such as the BC, the CFE and the Cabo Frio coastal upwelling.  
154 Following Calado et al. [2008], characteristic profiles from the BC inshore edge  
155 (TS-inshore), core (TS-core) and offshore edge (TS-offshore) were obtained

156 from this dataset to support the feature model conception. These profiles  
 157 Calado et al. [see Figure XX from 2008] shows that thermocline depths increase  
 158 towards the ocean interior. At the inshore edge, thermocline depths varies  
 159 between 20 and 70 meters, while at the offshore edge it ranges between 50  
 160 and 170 *m*. This the signature of the southward geostrophic transport from  
 161 the BC, and it's the desirable structure for the feature model. This dataset  
 162 contains the typical vertical structure of the features of interest, such as the  
 163 BC, and the cyclonic and anticyclonic eddies.

164 Once identified the features of interest, the next step was to build a bi-  
 165 dimensional grid to construct the Feature Models. The grid to construct the  
 166 BC Feature Model was defined along the BC path and thickness identified  
 167 from satellite SST imagery (Fig. 5). The grid is oriented in the cross-stream  
 168 (*X*) and along stream (*Y*) direction, with *Y* varying according to the me-  
 169 anderling of the current path. Similarly, the eddy Feature Model was built  
 170 using a circular grid that matched the identified position and diameter. In the  
 171 eddy grid, the *X* direction correspond to radial sections, while the *Y* direction  
 172 indicates the section's angular position.

173 Once the bi-dimensional grid is ready, parametrics functions are used to build  
 174 the Feature Model. First, the  $\varphi(z)$  function (Equation 1), which represents the  
 175 three non-dimensional profiles (TS-inshore, TS-core and TS-offshore), is used  
 176 to construct the BC Feature Model. From these three profiles, the TS-offshore  
 177 was filtered to match the surrounding July WOA'05 climatology profiles, which  
 178 is used as a background dataset in the Objective Analysis mapping technique  
 179 that is described next.

$$180 \quad \varphi_i(z) = \frac{T_i(z) - T_{i_b}}{T_{i_s} - T_{i_b}} \quad (1)$$

181 Second, the standard temperature and salinity dimensionless sections are ob-  
 182 tained by applying this non-dimensional profiles in the *X* direction. These sec-  
 183 tions have the characteristic horizontal gradient from a southward geostrophic  
 184 transport. With this, the Feature Model enables one to build the three-dimensional  
 185 structure of the current based on any surface tracer horizontal distribution us-  
 186 ing this relation:

$$187 \quad T_i(z) = [T_{i_s} - T_{i_b}] \varphi_i(z) + T_{i_b} \quad (2)$$

188 where the index *i* indicates the *X* position along the Feature Model section,  
 189 and subindices *s* and *b* refer to surface and bottom value of the hydrographic  
 190 tracer. At this step the surface tracer distribution was based on the July  
 191 WOA'05 climatology.

192 Third, to prescribe the cyclonic eddy, a similar technique based on dimen-

193 sionless profiles ( $\varphi(z)$ ) was employed using the equations proposed by Calado  
 194 et al. [2006].

195 The forth step consisted in merging the three dimensionless fields using Equa-  
 196 tion 3. An Objective Analysis scheme was applied to merge our synoptic BC  
 197 and anticyclonic eddy with the July WOA'05 1 degree background climatology.  
 198 In this phase, the resulting tri-dimensional field contains background clima-  
 199 tological conditions that were slightly modified to accomodate the synoptic  
 200 structure of the Feature Models. We designate this field as Feature Oriented  
 201 Models System (FORMS) (details available on Calado et al. [2008]).

$$202 \quad \varphi'_i(z) = [\varphi_{i=1,k}^{BC}(z); \varphi_{i=k+1,M}^{EDDY}(z); \varphi_{i=N+1,N}^{CLIM}(z)] \quad (3)$$

203 The fifth and last step consisted of transforming the dimensionless tri-dimensional  
 204 field into dimensional temperature and salinity fields by applying satellite SST  
 205 and WOA'05 surface salinity data at surface using Equation 4, respectively.  
 206 The resulting field contained the synoptic BC structure and it's associated  
 207 anticyclonic eddy Feature Models based on the July climatological distribu-  
 208 tion (Fig. 6). The final product is a three-dimensional initial conditions for  
 209 temperature and Salinity field, that accurately assimilate the SST conditions  
 210 attached to the FORMS structure (Fig. ??).

$$211 \quad T'_i(z) = [T_{i_s} - T_{i_b}] \varphi'_i(z) + T_{i_b} \quad (4)$$

### 212 3.3 The Numerical Model

213 Our numerical experiments were based on the Regional Ocean Modeling Sys-  
 214 tem (ROMS) v3.0 [Haidvogel et al., 2000; Shchepetkin and McWilliams, 2005].  
 215 ROMS is terrain following coordinate system model based on the hydrostatic  
 216 balance and oceanic primitive equations. This model solves the Reynolds av-  
 217 eraged form of the Navier Stokes equations and can be configured in several  
 218 different ways.

219 The model domain comprises the southeastern area of the Brazilian coast, be-  
 220 tween 19°S, 30°S, 35°W and 49°W, and it is tilted approximately 45° to match  
 221 the coastline orientation. Grid configurations were as follows: 172X172 points  
 222 evenly spaced every 1/12°, with forty vertical  $S$  ( $\sigma$ ) layers. The bathymetry  
 223 was derived from ETOPO-2, with gridded depths ranging between 10 and  
 224 4300 meters.

225 An open boundary condition scheme was also imposed on the northern, south-  
 226 ern and western limits employing radiation condition was applied to solve  
 227 the tracers and the baroclinic velocity component, a flather condition to the

228 barotropic component and a gradient condition to the free-surface. Wind forc-  
229 ing was not applied to simulations developed here, since we were interested  
230 in understanding the role of geostrophic flows in driving the formation and  
231 evolution of the mushroom-like eddy dipole.

232 Simulations were based on two different approaches following the concept de-  
233 veloped on Ezer and Mellor [1994]. For the nowcast experiment, ROMS was set  
234 to run in the diagnostic mode (flag *TS\_FIXED* defined), which allows one to  
235 compute the free-surface and momentum fields based on a fixed/non-evolving  
236 density structure. The objective of this methodology is to spin-up the model  
237 maintaining it's initial temperature and salinity conditions. To perform the  
238 ocean forecast, the model was setup in the prognostic mode (flag *TS\_FIXED*  
239 undefined). The prognostic run is based on the evolution of the mass field, and  
240 implies the prediction of the fluid state into the future. The prognostic run is  
241 initialized with the adjusted nowcast field, and a short-forecast of 5 days is  
242 performed (??)

## 243 4 Modeling Results

244 In this section, modeling outputs are assessed (i) to verify the model accu-  
245 racy in reproducing the oceanographic features commonly observed along the  
246 brazilian coast (section 4.1), (ii) to evaluate the evolution of the eddy dipole  
247 event of July 2006 (section 4.2), and (iii) to investigate the mechanisms driv-  
248 ing the formation and evolution of this mushroom-like eddy dipole in the BC  
249 (section 5).

### 250 4.1 The nowcast

251 - DESCREVER Figure 8

252 - DESCREVER Figure 9

253 Figure 7 shows the evolution of the averaged kinetic energy for the entire do-  
254 main. It is visible that the model energy rapidly peaks around  $1.6 \times 10^{-2} J/m^2$   
255 and then stabilizes at  $10^{-2} J/m^2$  after the third day. Within the first day of  
256 simulation, it is evident the establishment of a balance between the density  
257 field (pressure gradients) and the momentum field (coriolis force), while the  
258 kinetic energy grows. Figure 8 shows steps of the diagnostic run,. After two  
259 hours, surface velocity vectors point in the direction of the pressure gradient  
260 force. As the Coriolis force begins to balance the pressure gradient force, the  
261 resulting velocity is deflected to the left (6 and 8 hours) until it reaches a

262 stable position. Once the kinetic energy and the velocity field get stabilized,  
263 we have reached our Nowcast Field. When geostrophic balance is reached after  
264 three days of simulation, the nowcast field is obtained.

265 The Nowcast field is a thermohaline structure with satellite SST assimilated  
266 with fitted momentum structure for a synoptic behavior of the BC. The sur-  
267 face velocity field shows a meandering BC intimately associated to the SST.  
268 BC velocities range between  $0.5\text{ m/s}$  at the southernmost part of the domain  
269 and  $1.7\text{ m/s}$  at the eddy-dipole core, and the average value is around  $0.9\text{ m/s}$ .  
270 These values agree with previously reported data from direct current mea-  
271 surements [Müller et al., 1998], from geostrophic calculations [Campos et al.,  
272 1995; Silveira et al., 2004] and from modeling experiments [Campos et al.,  
273 2000; Calado et al., 2008; Fernandes et al., 2009].

274 At the CFE section a very interesting slice of the Nowcast field is seen (Fig. 9).  
275 On the coastal portion of the section a clear picture CFE is present. As ob-  
276 served, it's diameter reaches approximately 100 km and it's vertical structure  
277 is baroclinic-dominated. Silveira et al. [2004] described this baroclinic-eddy  
278 based on observations and highlighted it's distinct flow reversal with depths.

#### 279 4.2 The forecast

280 - DESCREVER Figure 10

281 Figure 10 shows the comparison between the evolution of model-derived versus  
282 satellite-derived SST. The comparison of the SST fields (model and satellite)  
283 provides a qualitative assessment showing that the evolution of the dipole and  
284 the position of the CB were reproduced by the simulation.

285 - COMPARAR com o altímetro aqui (Não consegui entender o que está escrito  
286 no parágrafo abaixo) The evolution of scenario that started by FORMS, with  
287 the visual analysis of the figures is clear the development of a mushroom-like-  
288 eddy in comparison with the satellite SST data, as observed on AVISOs data  
289 (Fig. 3 j,k,l).

290 The development of the mushroom from July, 23 to July, 28 present a stable  
291 structure that grows stationary on offshore area between Cabo Frio ( $23^\circ$ ) and  
292 São Paulo Basin ( $25^\circ$ ). At surface, the structure grows in the order of  $21\text{ /day}$ ,  
293 with the maximum length between the two cores about  $217\text{ km}$  measure at day  
294 26.

295 4.3 Eddy dipole dynamics

296 - DESCREVER Figure 11

297 - DESCREVER Figure 12

298 - DESCREVER Figure 13

299 The Figure 11 shows the potential vorticity at surface and the relative vorticity  
 300 surface fields. In the relative vorticity field is showed the section on mushroom,  
 301 that is shown on Figure 12 for relative vorticity over velocity meridional com-  
 302 ponent for days 23, 24 and 28 of july 2006. With these figures was possible to  
 303 identify, that after one day of simulation (day 24) the mushroom-like-eddy is  
 304 clear developed as a classic mushroom-like-eddy.

305 Figure 10 (c,d) and Figure 11 (c,d) show the cores of cyclonic and anticyclonic  
 306 eddies and the head of mushroom, enveloping the frontal part of the dipoles.  
 307 The Figure 12 for day 28 presents the configuration of 6 day evolution for the  
 308 mushroom-like-eddy, thats is reveals symmetric behavior for this structure.  
 309 The magenta lines is the zero relative vorticity values and the with lines a  
 310 zero velocities values. For the days 23 and 24 the symmetry is not clear, but it  
 311 can be confirmed as the dipole (mushroom) evolution as a dynamical coherent  
 312 structure.

313 Based on the study of Mied et al. 1991, is calculated the Rossby number ( $Ro$ )  
 314 and the ratio of the length scale to the internal deformation ratio  $\lambda = 2b/Rd$ ,  
 315 for the initial field on day 23. According the velocity field and the vorticity field  
 316 was possible extract the parameters to calculate  $\lambda$  and  $Ro$ . According with  
 317 the initial field the upper layer ( $H1$ ) is 400m and the lower layer limits,  $H2 =$   
 318 5000  $m$ . In this case was considered the dynamics of the BC as a two layers  
 319 system (Fernandes et al, 2009). The  $2b$  parameter, that measure the initial  
 320 length of core flux between the two initial eddies (cyclonic and anticyclonic),  
 321 for this case is 50  $km$ . Therefore, was using these parameters is calculate the  
 322 Internal Deformation Ratio ( $Rd$ ) according:

$$323 \quad Rd = \frac{1}{f} \left[ \frac{g' H1 H2}{H1 + H2} \right]^{\frac{1}{2}} ; \quad (5)$$

324 where,  $f$  is the coriolis parameter and  $g'$  is reduced gravity. With  $\lambda$  and  $Ro =$   
 325  $U/2bf$ , where  $U$  is 1.7  $m/s$ , is possible to find, according Mied et al. 1991, the  
 326 zones that the initial field can develop the stable, unstable or no mushroom  
 327 represent at Figure 13. The Figure 13, defines the region of formation evolution  
 328 for a mushroom-like-eddy. The unrealistic regions for the BC mushrooms,  
 329 corresponds a  $\lambda > 2.55$  and  $Ro < 1$ , thats means the first density layer is

330 lower than  $100\text{ km}$ . On the other hand, for  $\lambda < 1$  and  $Ro > 1$ , represents that  
331 the length of BC is lower than  $50\text{ km}$ . These cases was considered unrealistic  
332 for the BC system.

333 For the experiment, conducted in this article, the initial field should develop a  
334 stable mushroom-like-eddies, according the  $\lambda = 1.252\text{ m}$  and  $Ro = 3.9 \times 10^4\text{ m}$   
335 (Fig. 13 and Table 1). The symmetry evolution can be confirmed from the  
336 visual analysis of Figures 10, 11 and 12 . With the  $Ro, \lambda$  plane (Fig. 13), is easy  
337 to analysis the sensibility of the parameters  $2b, U$ , and  $Rd$  for the development  
338 of the mushrooms. For  $H1$  parameter, increase or decrease the mushroom will  
339 still be in the region of stable development. On the other words, when the  
340 depth of first density layer vary (Tab. 1), the  $\lambda$  varies on the  $Ro, \lambda$  plane.  
341 However, when those variation happens, those do not change the condition of  
342 stable mushroom. On the other hand, if the initial speeds ( $U$ ) increase, the  
343 mushroom development becomes asymmetric (Tab. 2). The comparison of the  
344 two tables can show that the case of  $H1$  variation, the density layer changes  
345 the  $g'$ ,  $Rd$  and  $\lambda$ , However, when the  $U$  varies only  $Ro$  change. In this case  
346 the condition of asymmetric mushroom-like-eddy are satisfy.

347 For an other asymmetric development case, is when  $2b$  parameter decreases  
348 significantly, therefore, that is unrealistic case, that means BC length is less  
349 than  $50\text{ km}$ . Then is possible the development of a asymmetric mushroom  
350 if the core of Brasil current is greater than  $2\text{ m/s}$ , and its path cross the  
351 isobaths. The first conclusion of this analysis shows that BC mushrooms, most  
352 of the time should develop a symmetric structures. The hypothesis for the BC  
353 mushroom develop a asymmetric structures, that the velocities can increase  
354 the horizontal shear and consequently the barotropic instabilities will increase,  
355 developing the unstables structures.

## 356 5 Discussion

357 - COMPARAR resultados quantitativos descritos na secao 5, com as informa-  
358 coes especificas das referencias que estao nos paragrafos abaixo.

359 - OS paragrafos abaixo sao

360 According to the analysis, based on parameters Rossby number ( $Ro$ ) and the  
361 ratio of the length scale to the internal deformation ratio  $\lambda$ , considering a  
362 two layer system, it was possible to confirm the evolution of a symmetrical  
363 mushroom-like-eddy, with a mean growth rate is  $21\text{ km/day}$ , thats correspond  
364 a  $0.048\text{ days}^{-1}$ . This growth rate corroborates with the values presents for the  
365 most untable wave growth rate decribe on Silveira et al. [2008], thats is about  
366  $0.045 - 0.06\text{ days}^{-1}$ . Also, the authors shows that this waves correspond a

367 wavelengths are within the 260 – 350 *km* range and are characterized by very  
368 low phase speeds compared to the surface BC velocity.

369 Mushrooms like currents or eddies, are possibly the most common structures  
370 in the ocean, according to an Fedorov and Ginsburg [1986]. In this article are  
371 discusses the various ways of forming these structures in the ocean. Essentially,  
372 the authors claims that horizontal shear, induced by current flows plays the  
373 principal role. However, these authors refer to these structures with vertical  
374 coherence of a few meters to a few tens of meters. In Fedorov et al. [1989],  
375 with studies in rotation tanks, it was discussed in more detail the formation  
376 of mushrooms like currents, based on the influence of Earth’s rotation. In  
377 this study, the authors explore how the  $\beta$ -plan and  $f$ -plan plays a role in  
378 the evolution and formation of mushrooms. The conclusions was appointed as  
379 the  $\beta$ -plan does not have a key role on these structures. Moreover, this study  
380 pointed out how the stratification can stabilizes the mushrooms structures  
381 after its formation.

382 From these fundamental works, Meid et al. [1991], with idealized numerical ex-  
383 periments in  $f$ -Plan , discussed the formation of mushrooms-like-eddies based  
384 on geostrophic scenario. These authors explain a symmetrical mushroom oc-  
385 cur when the Rossby number  $Ro$  is  $\leq 1$  or the range of deformation radius  
386 in  $\lambda$  structure  $\leq 0.5$ . However, the formation of an asymmetric structure  
387 of mushrooms occurs when  $Ro \geq 1$  and  $\lambda \geq 1$ , indicating that vorticity is  
388 dominated by the tikness water column. These authors, unlike Fedorov and  
389 Ginsburg [1986], tried to isolate numerically the formation conditions of these  
390 structures. It could reveal the importance of wind gradient swing the formation  
391 mechanism of mushrooms-like-eddies. Hookers and Brown [1996] discussed the  
392 formation of dipole vortices the possible evolution of mushrooms-like-eddies in  
393 the region of the confluence Brazil - Malvinas through remote sensing. These  
394 authors show that is evident how the interaction of boundary currents can  
395 form the bipolar structures. Therefore the dipoles are vortically more active  
396 than the isolated eddies. These authors also show that the dipoles can be  
397 formed by intense currents like the Gulf Stream and also by weak currents,  
398 such as the Brazil Current. This suggests that the formation of structures does  
399 not depend on the strength of the current.

400 Moreover, in the context of western boundarys Current, where often recurrent  
401 mushrooms-like-eddies are observed, it is necessary to deepen the discussion  
402 of geophysical instability. That is knowing [Silveira et al., 2008] the growth  
403 of primary meanders and eddies of western boundary Currents mechanisms.  
404 The study of Stern and Whitehead [1990], where coastline curvature along  
405 the path of western boundary Current jet passing an abrupt angle of coast  
406 break, similar that occur in Cabo Frio, it favors separation of the jet from the  
407 boundary and a mushroom-like-eddy form. The authors suggest the Barotropic  
408 instability is de mais mechanism for the formation of mushrooms as separation

409 jet.

410 The work Beron-Vera et al. [2008] through altimeter data and calculation  
411 of Lyapunov exponent, across the ocean as well, revealing how is common  
412 to the formation of mushroom-like-eddies. In this study, the authors shows  
413 the mushroom structures are only a few times larger than the first baroclinic  
414 deformation radius. This indicates a consistent idea on which these structures  
415 are the result of baroclinic instability, such as described on Stammer [1997];  
416 Scott and Wang [2005]. This process makes these structures may vigorously  
417 persist for tens of days or months.

418 On the other perspective, Miranda [2013] through idealized models, it was  
419 revealed that the formation of eddy pairs (dipoles) along BC seems to be  
420 an unstable wave train. In this work, however, it was isolated the effect of  
421 horizontal shear and consequently the role of Barotropic instability in the  
422 formation of dipoles. In this configuration the formation of mushroom-like-  
423 eddies is evident as the CB jet detaches from the coast, indicating that the  
424 formation of the bipolar structure is induced by Barotropic instability.

425 The formation and evolution of eddy dipole structures for mushroom-like-  
426 eddies setting, seems to rely heavily on the horizontal shear. Thus, we can  
427 think about questions such as: How can be the evolution of BC mushroom-  
428 like-eddy? In this study, we isolated a real scenario where the CB gives off the  
429 coast, forming initially one cyclonic meander, which evolves into a mushroom  
430 like eddy. The vertical structure of mushroom like current is clearly Baroclinic,  
431 revealing the complexity of forming of this structure. A possible Barotropic  
432 interaction and the induction of the Baroclinic balance turns the mushroom of  
433 opposite direction into sub-pycnoclinic depths. That is, the vertical structure  
434 of the mushroom formed on the CB frontal eddy has clear baroclinic signature  
435 [Calado et al. 2008; Silveira et al 2008; Calado et al 2010; Fernandes et al 2009].

## 436 **6 The final remarks**

437 - Essa secção deve descrever explicitamente os principais resultados desse estudo  
438 (liste alguns exemplos)

439 - Primeiro parágrafo sumariza o estudo e a motivação. Segundo parágrafo  
440 segue como "The main finding of this study is that Eddy dipoles in the BC  
441 behave as ...alguma coisa assim"

442 Alguns exemplos do que deve ser enfatizado

443 (a) This study revealed that eddy dipoles are a common feature linked with the

444 BC mesoscale variability. During 1993-2014, at least 62 events were identified  
445 using satellite altimetry data.

446 (b) Numerical simulations based on the FORMS technique captured the evo-  
447 lution of the dipole event of July 2006.

448 (c) Numerical simulations for the July 2006 event suggest that mean eddy  
449 dipoles in the BC behave as ....

450 (d) According to  $Ro$  and  $\lambda$  plane analysis, it is possible to conclude that in the  
451 region between Cabo Frio ( $23^\circ$ ) and the São Paulo Bight ( $25^\circ$ ) the probability  
452 is the occurrence of symmetrical mushroom-like-eddy.

## 453 **7 Acknowledgments**

454 The altimetry SSH products were produced by Ssalto/Duacs, distributed by  
455 AVISO, and supported by the CNES (available at: <http://www.aviso.oceanobs.com/>).  
456 We thank Conselho Nacional de Pesquisa e Desenvolvimento Tecnológico (CNPq)  
457 via grant XXXXXXXX/2016-1, the Instituto de Estudos do Mar Almirante  
458 Paulo Moreira / Marinha do Brasil (IEAPM/MB), The School of Marine Sci-  
459 ence and Technology / University of Massachusetts Dartmouth (SMAS/UMassD),  
460 Also ... Ricardo Domingues acknowledges support from the Cooperative In-  
461 stitute for Marine and Atmospheric Studies (CIMAS), University of Miami,  
462 and from the NOAA Atlantic Oceanographic and Meteorological Laboratory.

## 463 **References**

- 464 Calado, L., Gangopadhyay, A., da Silveira, I., 2006. A parametric model for  
465 the Brazil Current meanders and eddies off southeastern Brazil. *Geophysical*  
466 *research letters* 33 (12), L12602.
- 467 Calado, L., Gangopadhyay, A., Silveira, I., 2008. Feature-oriented regional  
468 modeling and simulations (FORMS) for the western South Atlantic: South-  
469 eastern Brazil region. *Ocean Modelling* 25 (1-2), 48–64.
- 470 Campos, E., Muller, T., Peterson, R., 1995. Physical oceanography of the  
471 southwest Atlantic Ocean. *Oceanography* 8 (3), 87–91.
- 472 Campos, E., Velhote, D., Silveira, I., 2000. Shelf break upwelling driven by  
473 Brazil Current cyclonic meander. *Geophys Res Let* 27 (2000), 751–754.
- 474 da Silveira, I., Lima, J., Schmidt, A., Ceccopieri, W., Sartori, A., Francisco,  
475 C., Fontes, R., 2008. Is the meander growth in the Brazil Current system  
476 off Southeast Brazil due to baroclinic instability? *Dynamics of Atmospheres*  
477 *and Oceans* 45 (3-4), 187–207.

- 478 Domingues, R., Goni, G., Bringas, F., Muhling, B., Lindo-Atichati, D., Wal-  
479 ter, J., 2016. Variability of preferred environmental conditions for Atlantic  
480 bluefin 1 tuna (*Thunnus thynnus*) larvae in the Gulf of Mexico during 1993-  
481 2011. *Fisheries Oceanography* in press.
- 482 Ezer, T., Mellor, G., 1994. Diagnostic and prognostic calculations of the North  
483 Atlantic circulation and sea level using a sigma coordinate ocean model. *J.*  
484 *Geophys. Res* 99 (14), 159–14.
- 485 Fernandes, A., da Silveira, I., L.Calado, Campos, E., Paiva, A., 2009. A two-  
486 layer approximation to the Brazil Current Intermediate Western Boundary  
487 Current System between 20S and 28S. *Ocean Modelling* 29 (2), 154–158.
- 488 Fox, D., Carnes, M., Mitchell, J., 1992. Characterizing major frontal systems:  
489 A nowcast/forecast system for the Northwest Atlantic. *Oceanography* 5 (1),  
490 49–53.
- 491 Gangopadhyay, A., Lermusiaux, P., Rosenfeld, L., Robinson, A., Calado, L.,  
492 Kim, H., Leslie, W., Haley, P., 2011. The California Current System: A mul-  
493 tiscala overview and the development of a feature-oriented regional modeling  
494 system (FORMS). *Dynamics of Atmospheres and Oceans* 52 (1-2), 131–169.
- 495 Gangopadhyay, A., Robinson, A., 2002. Feature-oriented regional modeling of  
496 oceanic fronts. *Dynamics of Atmospheres and Oceans* 36 (1-3), 201–232.
- 497 Gangopadhyay, A., Robinson, A., Arango, H., 1997. Circulation and dynamics  
498 of the western North Atlantic. Part I: Multiscale feature models. *Journal of*  
499 *Atmospheric and Oceanic Technology* 14 (6), 1314–1332.
- 500 Garfield, N., 1990. The brazil current at subtropical latitudes. Ph.D. thesis,  
501 University of Rhode Island, 121 pp.
- 502 Haidvogel, D., Arango, H., Hedstrom, K., Beckmann, A., Malanotte-Rizzoli,  
503 P., Shchepetkin, A., 2000. Model evaluation experiments in the North At-  
504 lantic Basin: simulations in nonlinear terrain-following coordinates. *Dynam-*  
505 *ics of Atmospheres and Oceans* 32 (3-4), 239–281.
- 506 Lorenzetti, J., Stech, J., Mello Filho, W., Assireu, A., 2009. Satellite obser-  
507 vation of Brazil Current inshore thermal front in the SW South Atlantic:  
508 Space/time variability and sea surface temperatures. *Continental Shelf Re-*  
509 *search*.
- 510 Müller, T., Ikeda, Y., Zangenberg, N., Nonato, L., 1998. Direct measurements  
511 of western boundary currents off Brazil between 20 S and 28 S. *J. Geophys.*  
512 *Res* 103, 5429–5437.
- 513 Robinson, A., Glenn, S., 1999. Adaptive sampling for ocean forecasting. *Naval*  
514 *Research Reviews* 51 (2), 26–38.
- 515 Robinson, A., Spall, M., Pinardi, N., 1988. Gulf Stream simulations and the  
516 dynamics of ring and meander processes. *J. Phys. Oceanogr* 18 (12), 1811–  
517 1854.
- 518 Schmid, C., Schäfer, H., Podestà, G., Zenk, W., 1995. The Vitória eddy and  
519 its relation to the Brazil Current. *Journal of physical oceanography* 25 (11),  
520 2532–2546.
- 521 Shchepetkin, A., McWilliams, J., 2005. The regional oceanic modeling sys-  
522 tem (ROMS): a split-explicit, free-surface, topography-following-coordinate

523 oceanic model. *Ocean Modelling* 9 (4), 347–404.  
524 Silveira, I., Calado, A., Castro, B., Cirano, M., Lima, J., Mascarenhas, A.,  
525 2004. On the baroclinic structure of the Brazil Current–Intermediate West-  
526 ern Boundary Current system at 22–23 S. *Geophys Res Let* 31.  
527 Silveira, I., Campos, A., Campos, E., Godoi, S., Ikeda, Y., 2000. A corrente do  
528 Brasil ao largo da costa leste brasileira.[The Brazil current off the eastern  
529 brazilian coast]. *Revista Brasileira de Oceanografia* 48 (2), 171–183.  
530 Soutelino, R., da Silveira, I., Gangopadyay, A., Miranda, J., 2011. Is the Brazil  
531 Current eddy-dominated to the north of 20S? *Geophys Res Let* 38 (3),  
532 L0360.

Table 1

Table of condition for symmetric or asymmetric mushroom-like-eddy, according the variation of the  $H1$  thickness for the first density layer. The parameter  $2b = 50 \text{ km}$ .

|           | <b>H1 = 100 m</b>           | <b>H1 = 200 m</b>           | <b>H1 = 400 m</b>           |
|-----------|-----------------------------|-----------------------------|-----------------------------|
| <b>g'</b> | $0.012 \text{ m/s}^2$       | $0.013 \text{ m/s}^2$       | $0.014 \text{ m/s}^2$       |
| <b>Rd</b> | $1.9 \times 10^4 \text{ m}$ | $2.7 \times 10^4 \text{ m}$ | $3.9 \times 10^4 \text{ m}$ |
| $\lambda$ | $2.624 \text{ m}$           | $1.799 \text{ m}$           | $1.252 \text{ m}$           |
| <b>Ro</b> | $0.614 \text{ m}$           | $0.614 \text{ m}$           | $0.614 \text{ m}$           |

Table 2

Table of condition for symmetric or asymmetric mushroom-like-eddy, according the variation of the  $U$ . In this cas the thickness for the first density layer  $H1 = 400\ m$  and the parameter  $2b = 50\ km$ .

|           | $U = 1\ m/s$         | $U = 1.7\ m/s$       | $U = 2.7\ m/s$       |
|-----------|----------------------|----------------------|----------------------|
| $g'$      | $0.014\ m/s^2$       | $0.014\ m/s^2$       | $0.014\ m/s^2$       |
| $Rd$      | $3.9 \times 10^4\ m$ | $3.9 \times 10^4\ m$ | $3.9 \times 10^4\ m$ |
| $\lambda$ | $1.252\ m$           | $1.252\ m$           | $1.252\ m$           |
| $Ro$      | $0.351\ m$           | $0.614\ m$           | $0.948\ m$           |

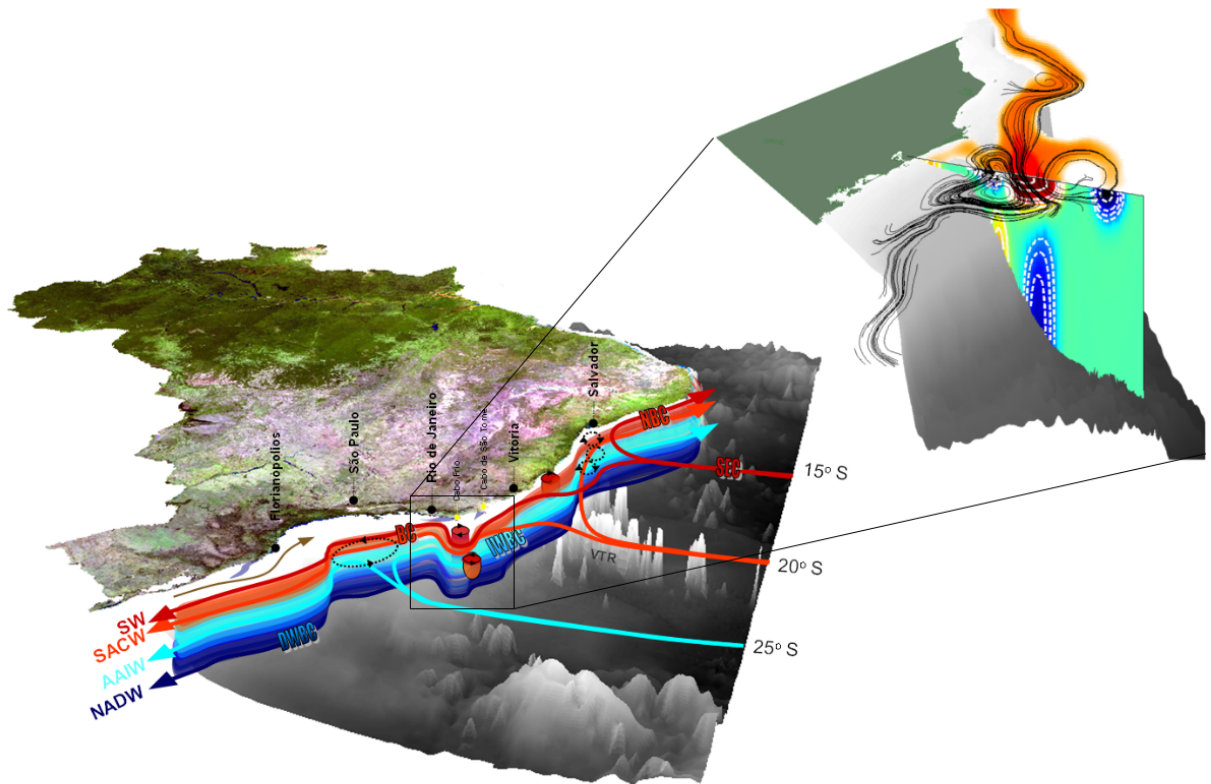


Fig. 1. Schematic circulation on the Brazilian coast and its associated bottom topography. Solid arrows show major currents while dashed arrows means possible recirculation cells. The colored gradient presents the main oceanic water masses present in the domain. Mesoscale features such as eddies, dipoles and upwelling regions are also illustrated. The upper panel is the zoom at mushroom development area, it shows the cross section mushroom-like-eddy feature.

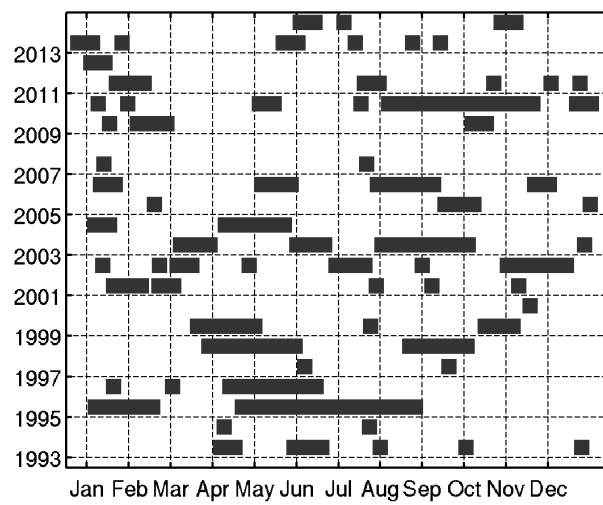


Fig. 2. Table with the occurrence of dipoles near Cabo Frio between 1993 to 2014. The eddy dipole events identified at the BC region using satellite altimetry data. Individual bars indicate timing and duration of each event. Total of 62

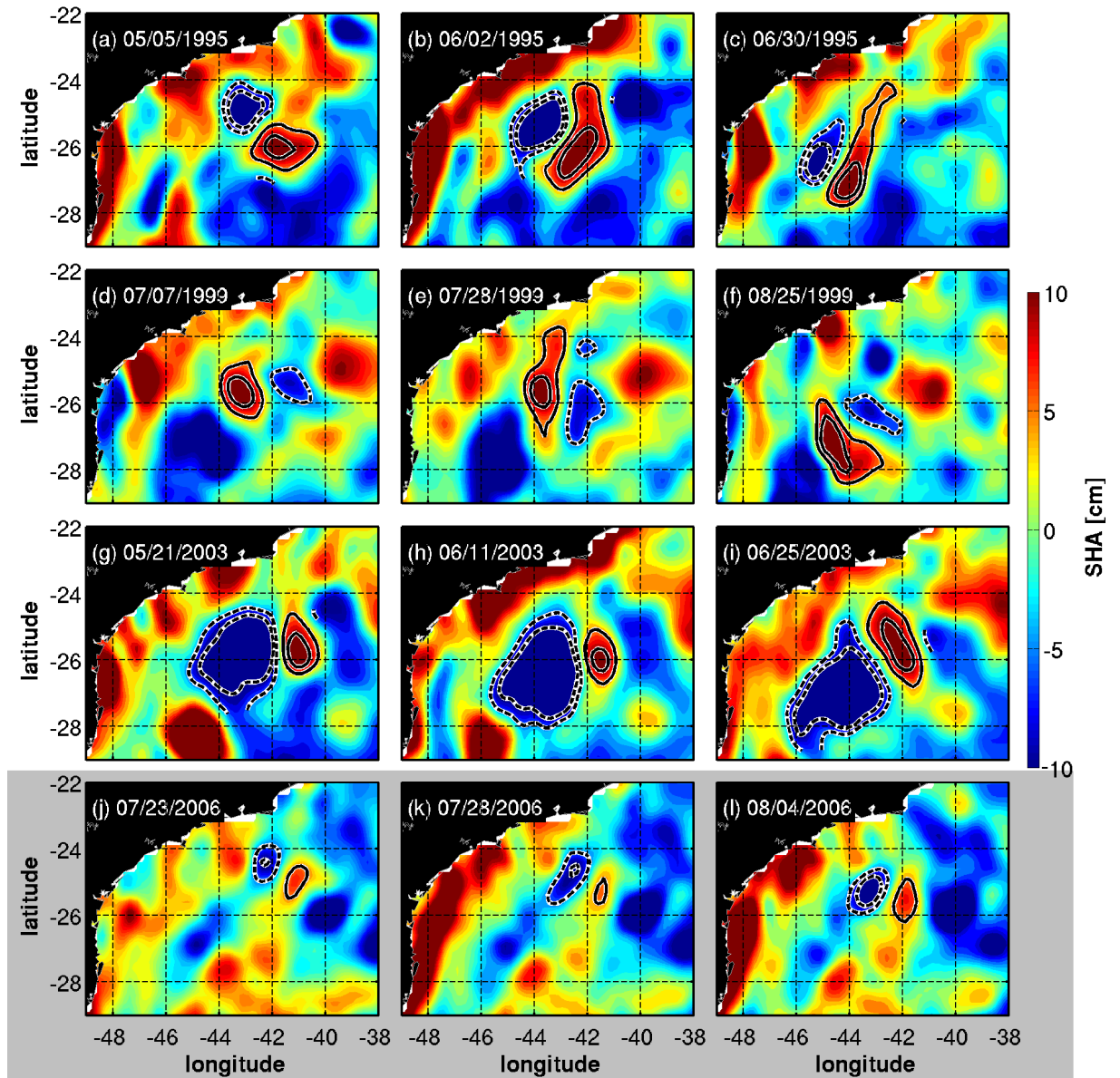


Fig. 3. Cabo Frio AVISO SSH data. Examples of eddy dipole features at the BC as identified using satellite-derived SHA data. The last three panels highlighted by the gray shading emphasize the event of July 2006, which is the focus of this study.

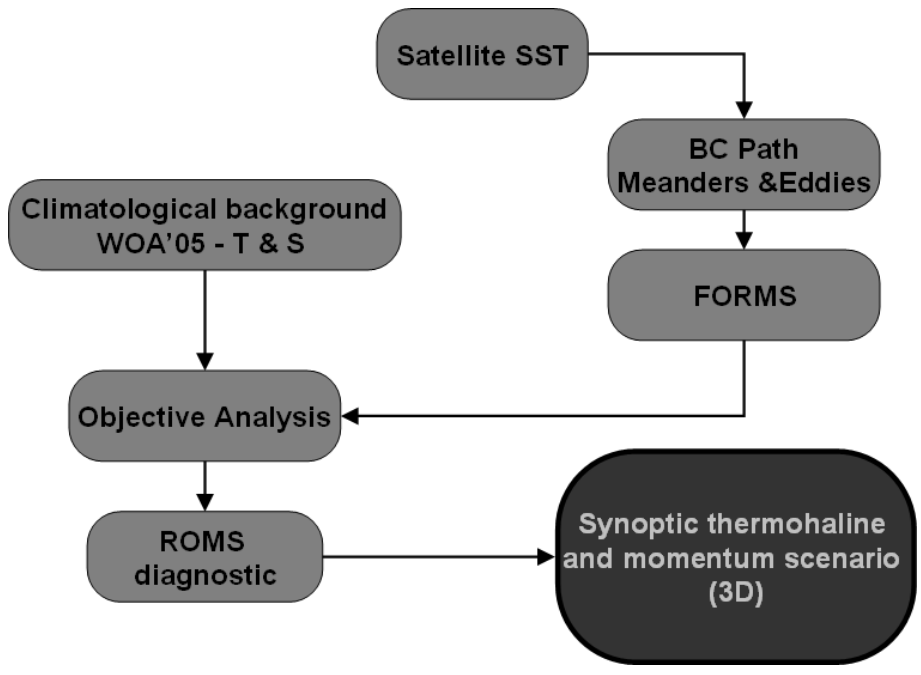


Fig. 4. Metodology of the present FORMS for the BC nowcast Simulation

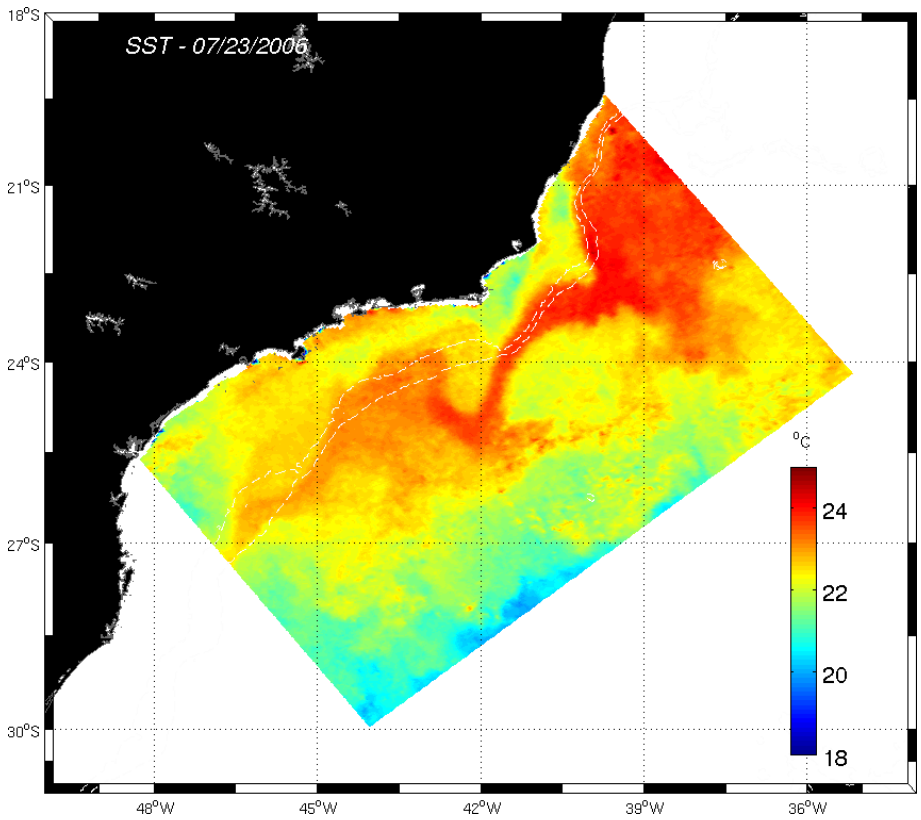


Fig. 5. Sea Surface Temperature for July 23, 2006.

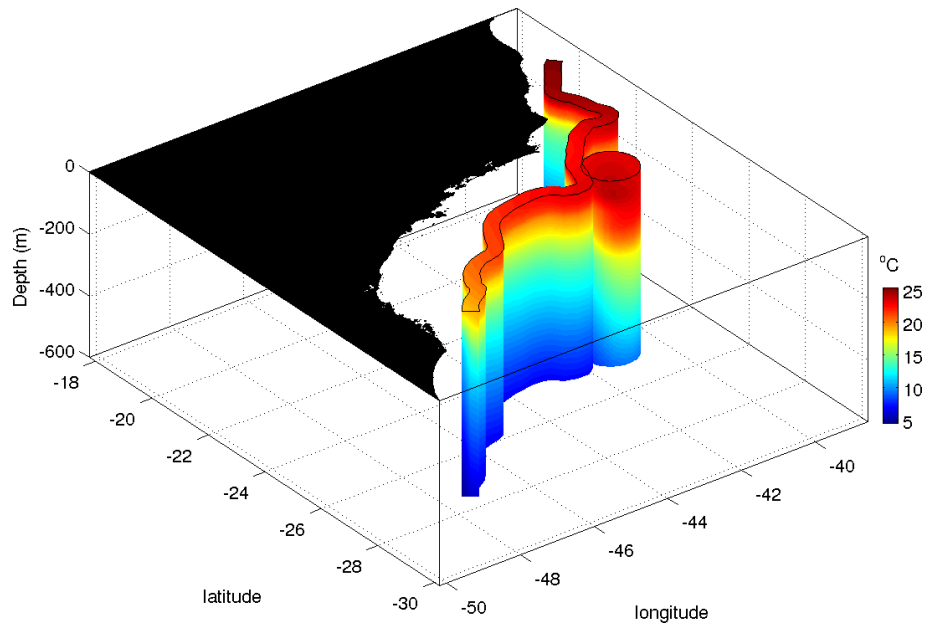


Fig. 6. Individual Temperature based Features Models 3D representation for BC and a Anticyclone Eddy at Cabo Frio region.

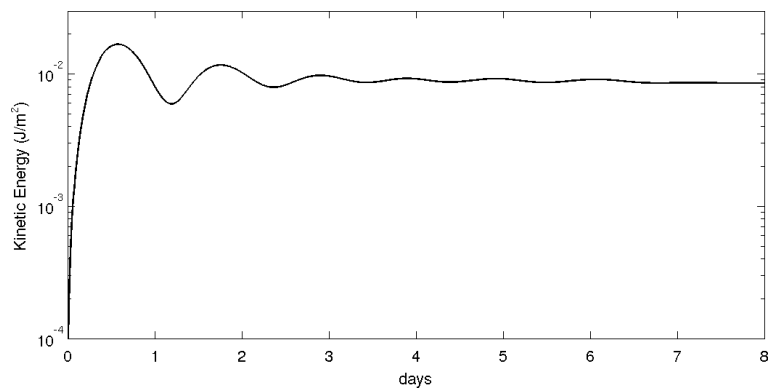


Fig. 7. Kinetic energy evolution. the energy can show how the FORMS scheme can stabilize the model. The results can be observer after few hours before the forecast initialize.

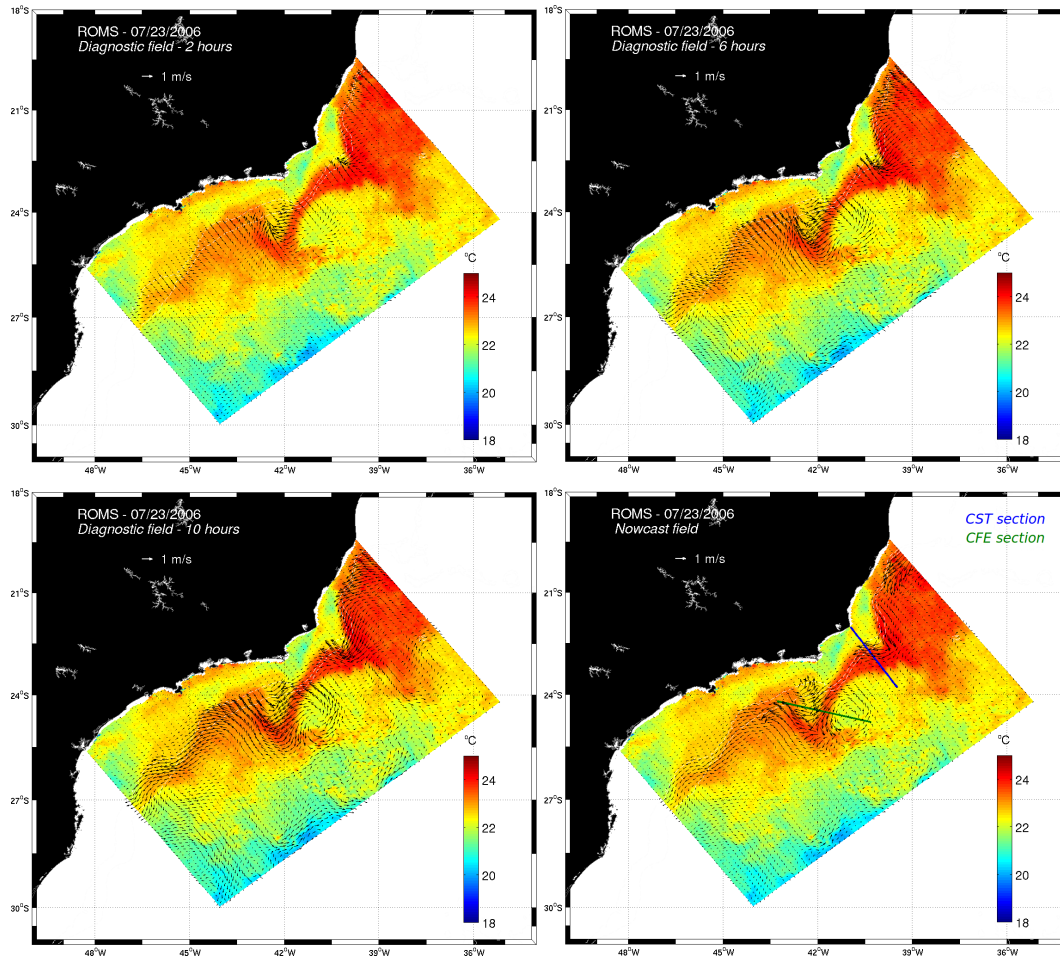


Fig. 8. FORMS diagnostic outputs showing the balance development and the resulting Nowcast field.

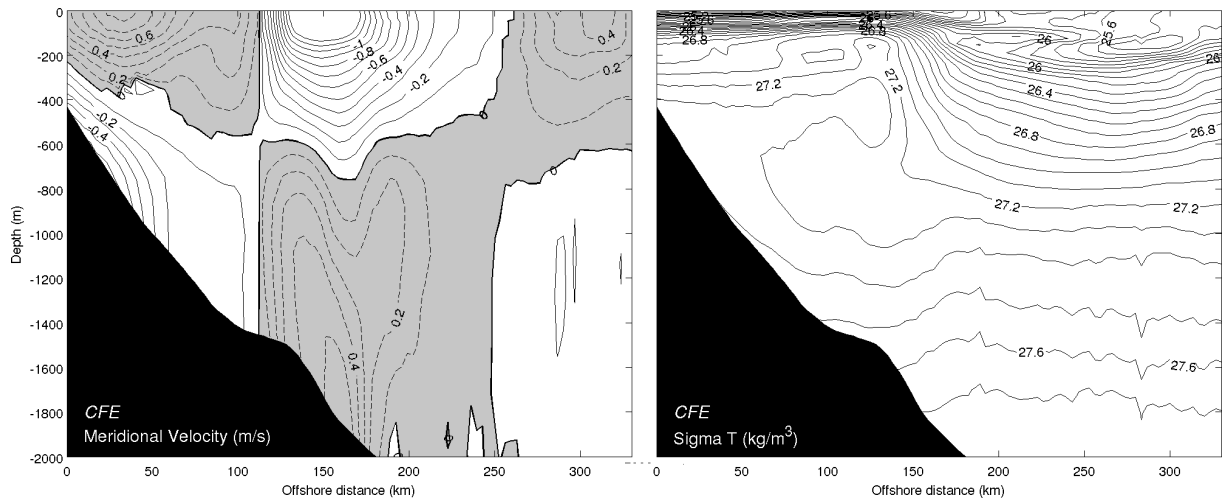


Fig. 9. Velocity cross section on the initial field.

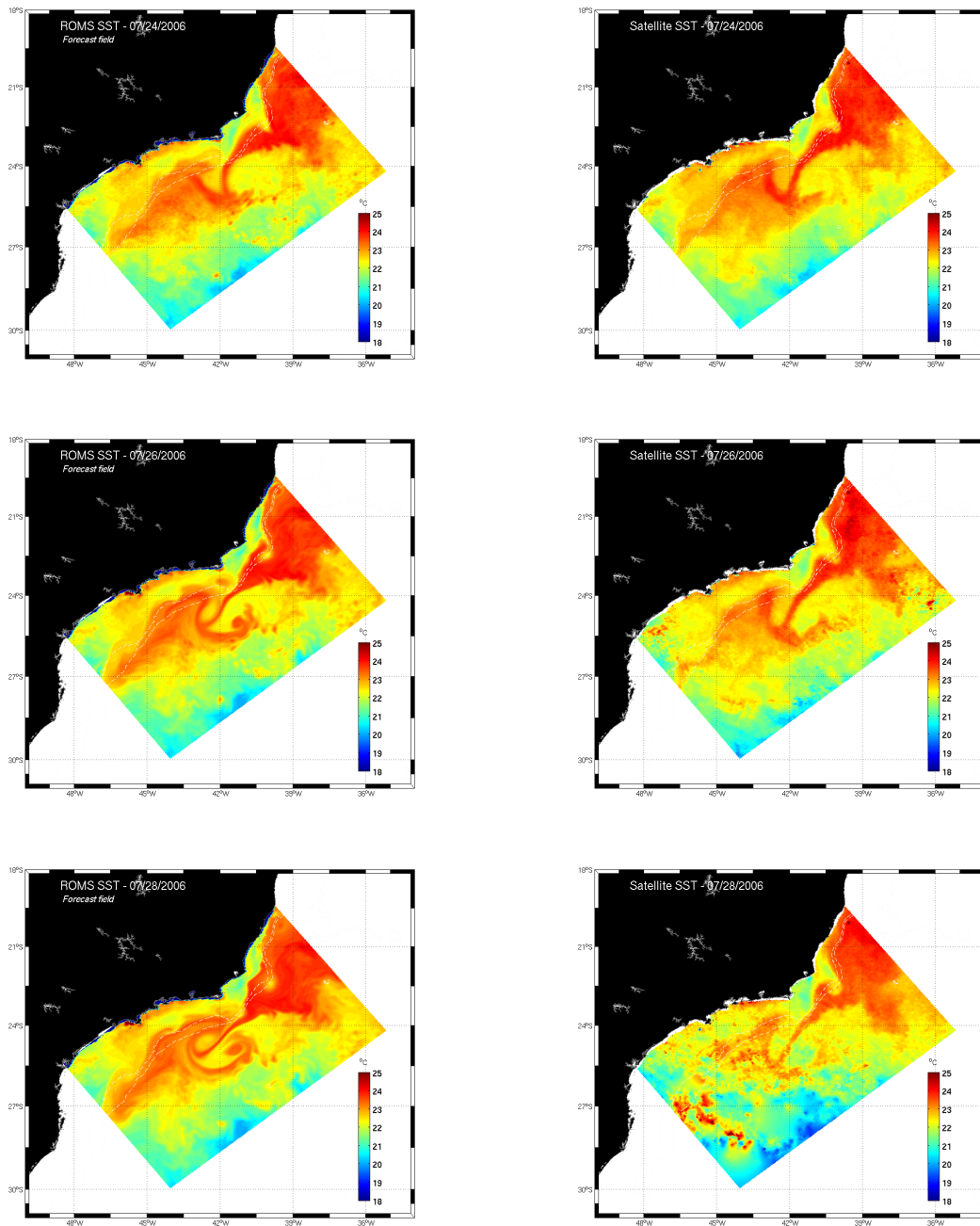


Fig. 10. SST forecasting. The left panel is the model forecasting SST field and the right panels is the SST from satellite based on OSTIA blended product.

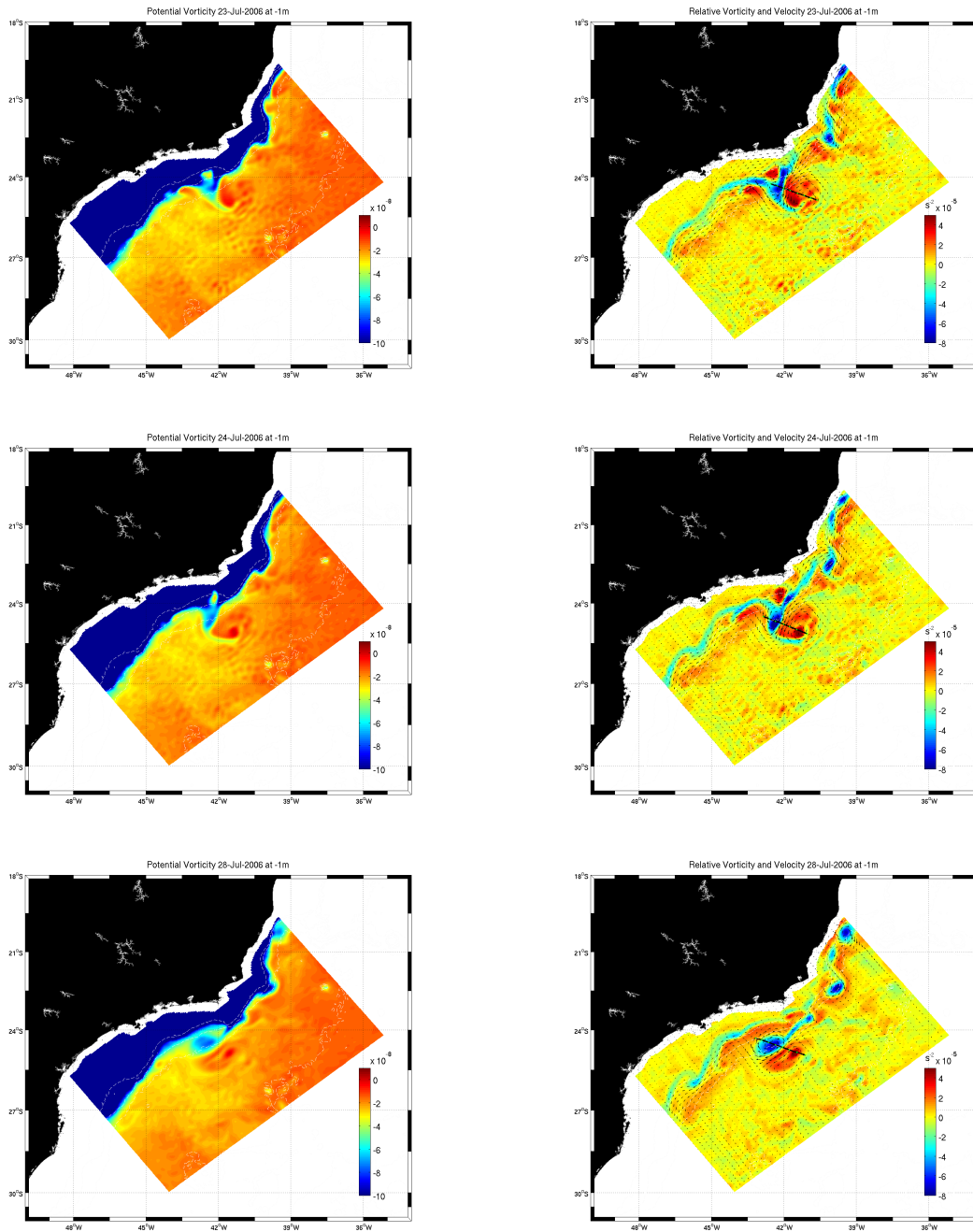


Fig. 11. Surface Potential vorticity field, Surface Relative vorticity for days 23, 24 and 28 of July 2006

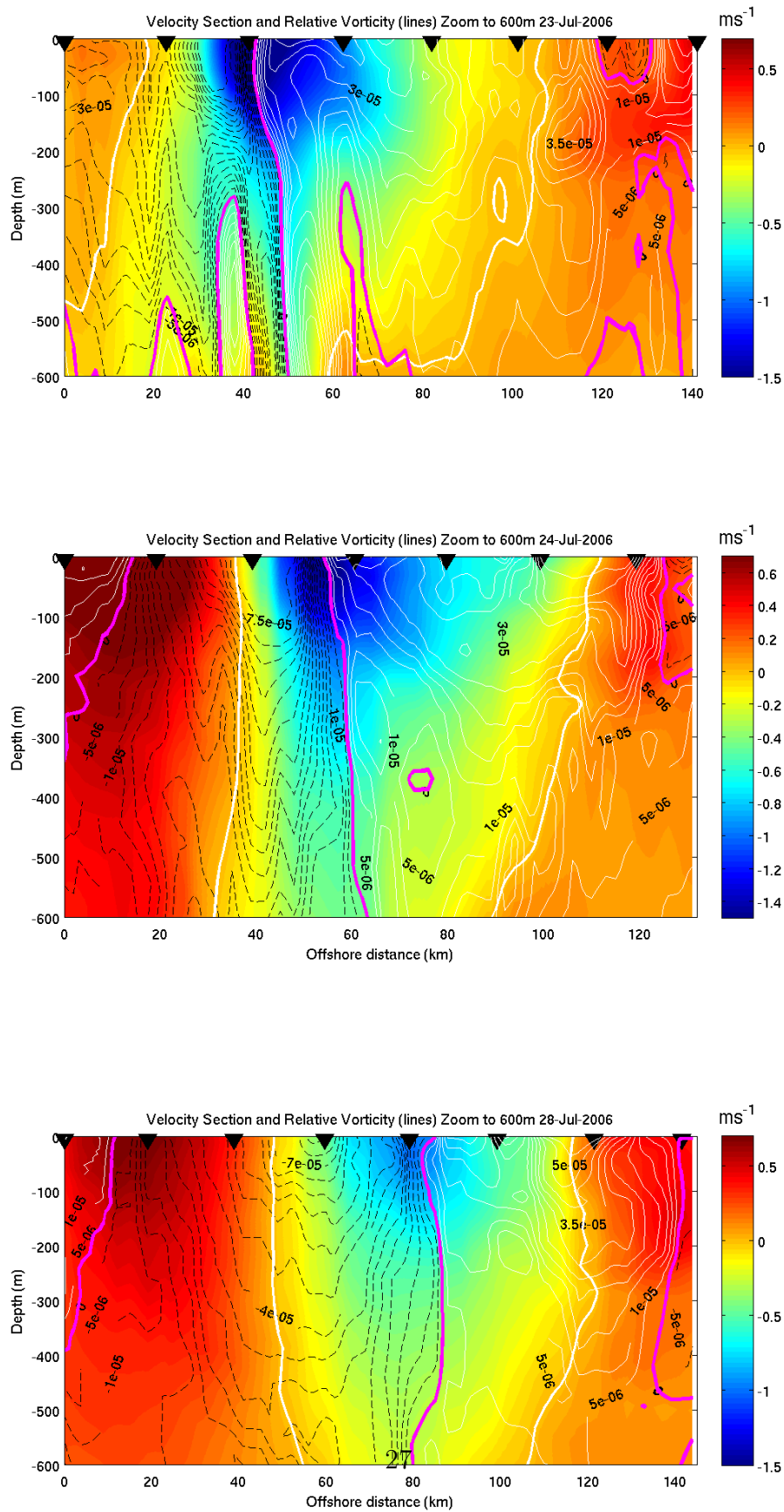


Fig. 12. Section of Relative vorticity (lines) over velocity on the mushroom-like-eddy. The zero vorticity are highlights by the magenta lines and the zero velocities are highlights by white lines.

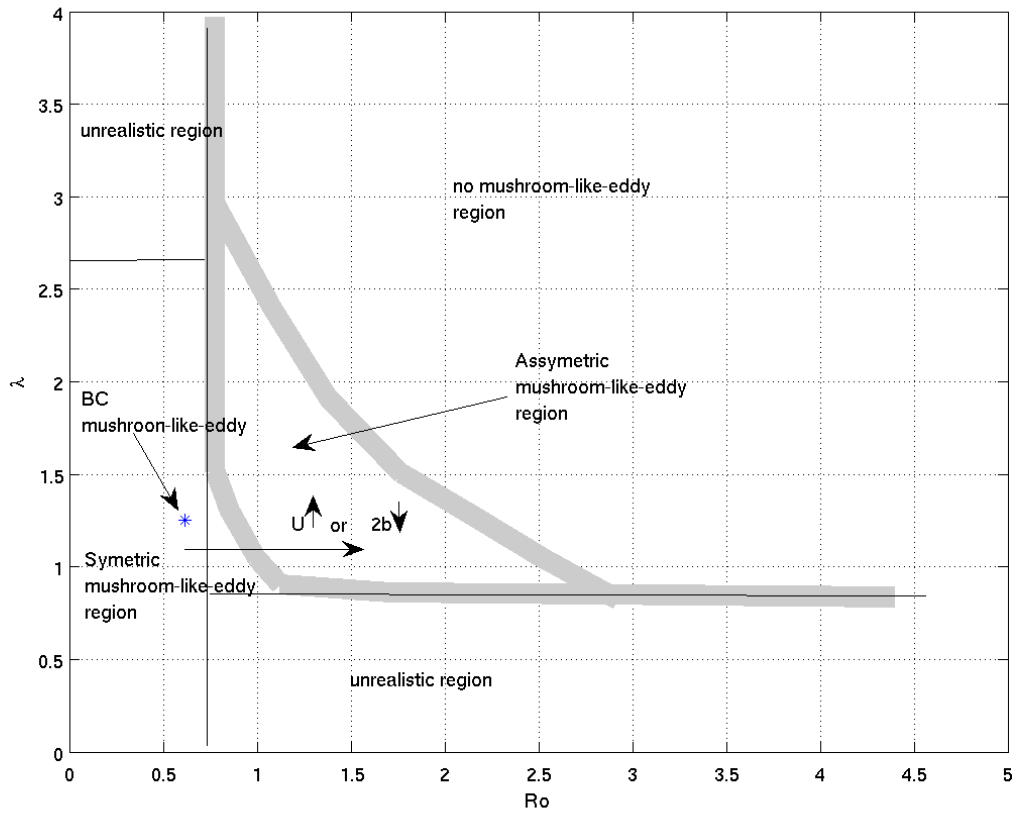


Fig. 13.  $Ro$  and  $\lambda$  plane. For the BC exeriment the  $Ro = 0.6142$   $m$  and  $\lambda = 1.2520$   $m$ . The paramters for the initial field is:  $H1 = 400$   $m$ ,  $H2 = 5000$   $m$ ,  $2b = 50$   $km$ ,  $g' = 0.0140$   $m/s^2$ ,  $Rd = 3.9 \times 10^4$   $m$